Published in final edited form as:
NMR Biomed. 2012 November ; 25(11): 1263–1270. doi:10.1002/nbm.2797.

Diffusion Tensor Quantification and Cognitive Correlates of the Macrostructure and Microstructure of the Corpus Callosum in Typically Developing Children and Dyslexics

Khader M. Hasan[1,*], **David L. Molfese**[2], **Indika S. Walimuni**[1], **Karla K. Stuebing**[3], **Andrew C. Papanicolaou**[4], **Ponnada A. Narayana**[1], and **Jack M. Fletcher**[2]

[1]Department of Diagnostic and Interventional Imaging, University of Texas at Houston

[2]Department of Psychology, University of Houston, Houston, Texas, United States of America

[3]Texas Institute for Measurement Evaluation and Statistics, University of Houston

[4]Department of Pediatrics University of Texas Health Science Center at Houston, Houston, Texas, United States of America

Abstract

Noninvasive quantitative magnetic resonance imaging methods such as diffusion tensor imaging (DTI), can offer insights into structure/function relationships in human developmental brain disorders. In this report, we quantified macrostructural and microstructural attributes of the corpus callosum (CC) in children with dyslexia and typically developing readers of comparable age and gender. Diffusion anisotropy, mean, radial and axial diffusivities of cross-sectional CC sub-regions were computed using a validated DTI methodology. The normalized posterior CC area was enlarged in children with dyslexia compared to typically developing children. Moreover, the callosal microstructural attributes, such as mean diffusivity of the posterior middle sector of the CC, significantly correlated with measures of word reading and reading comprehension. Reading group differences in FA, MD, and RD were observed in the posterior CC (CC5). This study demonstrates the utility of regional DTI measurements of the CC in understanding the neurobiology of reading disorders.

Keywords

diffusion tensor imaging; corpus callosum; microstructure; macrostructure; healthy; children; development; dyslexia; reading disorders; Letter Word ID; passage comprehension

INTRODUCTION

The corpus callosum (CC) is the largest interhemispheric commissural white matter bundle in humans with an estimated fiber density of 1 million axons per mm^2 (1, 2). Neocortical connectivity (3, 4) and age-related changes in area and volume of the CC are well documented across the human lifespan (5–12). The anterior CC, or genu, is populated by thinly myelinated, small-caliber axons that connect the frontal lobes (1, 11). The truncus, or middle CC, is populated by myelinated, large-caliber axons connecting the supplementary motor and auditory cortices. The posterior CC, or splenium, is populated by a mixture of

[*]Corresponding Author: Khader M. Hasan, Ph.D., Associate Professor of Diagnostic and Interventional Imaging, Department of Diagnostic and Interventional Imaging University of Texas Medical School at Houston, 6431 Fannin Street, MSB 2.100, Houston, Texas 77030, United States of America, Tel: Office (713) 500-7690, Fax: (713) 500-7684, Khader.M.Hasan@uth.tmc.edu.

medium and large, heavily myelinated axons that connect the temporal, parietal, and occipital cortices (12).

The consistent architectonics of the CC makes it a landmark uniquely sensitive to microstructural variation resulting from abnormal brain development or brain injury (13, 14). This attribute has been utilized extensively to identify neuroimaging markers for a host of applications that include cognitive (18–24), developmental (25–27), and neurodegenerative disorders (28, 29). In particular, structural alterations in CC have been identified in both developmental (e.g., dyslexia) and acquired (e.g., alexia) reading disorders (30–36).

Dyslexia affects an estimated 5–17% of school-aged children (37, 38). Despite numerous neuroimaging studies of both children and adults with dyslexia, the underlying neural substrates of reading disabilities remain elusive (39–41). Converging lines of evidence from perfusion, metabolic, functional, and anatomical MRI studies of reading implicate numerous left hemisphere structures in processing both written and spoken language (41, 42). However, a hallmark of the dyslexic brain is increased activation in the right hemisphere, especially in posterior regions (43). Given that the CC plays a major role in interhemispheric communications (1, 2, 19), the bilateral brain activations observed in dyslexics suggests possible changes in CC connectivity. Thus far, the CC literature on dyslexia is inconsistent and contains numerous contradictions (see 41 for review); possibly due to population definitions and disease heterogeneity of children with reading disabilities or because of poor CC tissue segmentation methods and uncontrolled age effects (5–12, 15–17).

We hypothesized that the macro- and microstructural attributes of the CC would offer insights into the inter-hemispheric communication in children with reading disabilities. To test this hypothesis we utilized a recently described and validated DTI-based tissue segmentation approach (8, 9) to identify macro- and microstructural properties of the midsagittal CC. We then compared properties of the CC in typically reading children with an age-matched cohort of children from two distinct reading disabled populations: children with letter and word decoding deficits (dyslexia) and children with fluency/comprehension deficits, but no decoding difficulties.

METHODS

Participant Demographics

Fifty children aged 10.5 to 16 years (mean = 13.4; S.D. = 1.2 years) gave written assent along with informed parental or guardian consent to participate in this study in accordance with the University of Texas at Houston institutional review board regulations for the protection of human subjects. Twenty-seven participants were male and 45 were right-handed (Table 1). All participants were English-speaking and identified as neurologically normal by review of medical history at the time of assessment.

Cognitive Scores

Children were administered a series of reading evaluations, including, the Woodcock-Johnson III Letter-Word ID and Passage Comprehension sub-tests (43, 44) to evaluate word reading and the Test of Word Reading Efficiency (TOWRE) (45) as a measure of reading fluency. In most participants, intelligence was measured using the Kaufman Brief Intelligence Test-2 (46) or the Stanford Binet Intelligence Test-4 (47). Based on their standardized test performance, children were assigned to one of three reading groups: typically-developing readers (TDR or controls), dyslexic readers (DX or dyslexics), or readers with comprehension or fluency problems (CF or Comprehension/Fluency). Children were classified as DX based on a standardized score below 90 on the WJIII word reading

test. The CF group fell below a 90 cutoff on the TOWRE and/or Woodcock Johnson III Passage Comprehension, but not on the WJIII Letter Word ID test. Typical readers scored above 90 on all tests. All children had IQ scores greater than 70 to rule out intellectual disabilities. In total, 24 children (11F) were categorized into the DX group, 15 (9F) into the group with CF deficits, and 11 (3F) as TDR. Means and standard deviations Letter Word ID and Passage Comprehension scores are presented in Table 1. TOWRE reading scores were unavailable for some TDRs, but other reading scores showed average or better levels of performance.

Conventional MRI and DWI Data Acquisition

We acquired whole-brain MRI data using a Philips 3.0 T Intera system with a SENSE parallel imaging receive head coil (Philips Medical Systems, Best, Netherlands). The MRI protocol (8,9) included (a) conventional MRI (3D spoiled gradient-echo (SPGR), field-of-view=240 mm x 240 mm (isotropic voxel size = 0.9375 mm), (b) 2D dual spin-echo images with echo/repetition times of $TE_1/TE_2/TR$=10/90/5000 ms, in the axial plane (44 axial slices, 3 mm thickness, 0 gap covering the entire brain from foramen magnum to vertex) (c) and a phase-sensitive MRI in the sagittal and axial planes, in addition to a matching volume of diffusion-encoded data as described below.

The diffusion-weighted image (DWI) data were acquired using a single-shot spin echo diffusion sensitized echo-planar imaging (EPI) sequence with the balanced *Icosa21* encoding scheme with twenty-one uniformly distributed orientations (48)**,** a diffusion sensitization or b-factor of 1000 $sec.mm^{-2}$, a repetition and echo times of TR=6100 ms, TE= 84 ms, respectively. EPI distortion artifacts were reduced by using a SENSE acceleration factor or k-space undersampling value of two (R=2). Spatial coverage matched the conventional MRI sequences described above (e.g., 44 axial sections, 3mm slice thickness and 0 mm gap with identical field-of-view). DTI acquisition time was approximately 7 minutes and resulted in signal-to-noise-ratio SNR-independent DTI-metric estimation (49).

DTI Processing

The DWI data were masked to remove non-brain tissue, image distortion-corrected and processed as described elsewhere (8). The intracranial volume (ICV) was computed from the masked T2-weighted volumes to account for brain size variability (9). In this work, the DTI-derived rotationally-invariant scalar metrics included the axial diffusivity ($\lambda_{||} = \lambda_1$), radial diffusivity ($\lambda_{\perp} = (\lambda_2 + \lambda_3)/2$), fractional anisotropy (FA) and mean diffusivity ($D_{av} = (\lambda_{||}+2*\lambda_{\perp})/3$).

Segmentation of the Corpus Callosum and its Subdivisions

The midsagittal CC identification procedure, validation and application across the human lifespan are detailed elsewhere (8). In brief, the identification of the midsagittal CC was based on the appearance of the inter-thalamic mass and the fornix on the isotropically interpolated DTI maps (8, 9). The CC was then segmented on the midsagittal slice using D_{av}, FA and the principal eigenvector (8, 9). The segmented CC was then subjected to a geometry-based subdivision into seven segments as described by Witelson (18): CC1-rostrum, CC2-genu (or gCC), CC3-rostral midbody, CC4-anterior midbody (or bCC), CC5-posterior midbody, CC6-isthmus and CC7-splenium (see Fig. 1A). Because CC1 showed more anatomic variation between subjects, we report findings for CC2 through CC7 and the entire midsagittal corpus callosum (eCC) which is defined as the sum of all callosal midsagittal sections including CC1. The DTI metric mean value of the midsagittal eCC was taken as the CC subregional area-weighted average.

Statistical Analysis

All analyses of callosal midsagittal cross-sectional areas and the corresponding DTI metrics variation were conducted in SAS 9.2 using PROC GLM (SAS Institute, Inc., 2008). All measures of CC area were normalized by the $ICV^{(2/3)}$ (8, 9). The corpus callosal midsagittal area (CCA), and ICV-normalized CCA and corresponding DTI metrics were modeled (fitted): $y_f = \perp_0 + \perp_1 * age$, then least-squares optimization methods were used to estimate the coefficients, standard deviations and their statistical significance using ANOVA. Spearman correlations of CC attributes with reading scores were then calculated with age as a covariate (50). Given a sample size of 50 (including 45 right-handers) and three reading groups, potential effects of gender and handedness were not analyzed, although previous studies on healthy controls did not identify gender differences (8, 9). Additional statistical analyses of data scatter were conducted using MATLAB R12.1 Statistical Toolbox v 3.0 (The Mathworks Inc, Natick, MA).

RESULTS

Group Comparisons between Subregional and Entire CC Areas

Representative **CC** segmentations from the three groups along with the anatomical midsagittal view are shown in Fig. 1B on three representative subjects from each group. Figure 2A shows a bar plot of the reading group average values and corresponding standard deviations and comparisons between the CC subregions (CC2-CC7) and entire CC areas of the TR, DX, and CF groups. Figure 2b shows the ICV-normalized CC areas ($nCCA=CCA/ICV^{2/3}$) to minimize brain size variability. Note that the splenium of the CC is the only region that is significantly larger in reading-disabled compared to controls ($p=0.024$). The reading subgroups did not significantly differ on area measurements on CC2-CC4 ($p>0.26$), but there is a trend towards a larger normalized corpus callosum in CC5 that did not achieve the critical level of alpha adopted for the study ($p=0.065$).

Group Comparisons between Subregional and Entire CC DTI Metrics

No significant group differences in mean diffusivity across the entire CC was observed ($p>0.12$; Fig 2C). The average FA(CC5) was significantly greater in DX compared with TDR (Fig. 2D; $p=0.024$), which is explained by a reduction in RD (Fig. 2D; $p =0.05$) and intact AD (Fig. 2E; $p=0.54$). The CF group did not differ from TDR on the callosal microstructural attributes.

Analysis of Covariance of the Individual CC Segments

The segments of the midsagital CC were analyzed separately. FA, MD, AD, RD and CC areas were compared between the TDR, DX, and CF groups. Age was included as a covariate in all models. In the genu (CC2), significant interactions between age and reading group were observed for both MD $F(2,44)=3.97$, $p<0.03$) and AD $F(2,44)=3.29$, $p<0.05$). Planned reading group comparisons were performed for both DTI metrics. MD for the TDR and CF groups differed $F(1,44)=8.19$, $p<0.007$) with CF children exhibiting higher MD. No other differences in MD were observed in CC2. When AD was compared, the TDR and DX reading groups did not differ, but approached significance $F(1,44)=3.91$, $p=0.055$). However the DX and CF groups were significantly different $F(1,44)=5.28$, $p<0.03$) wherein DX readers had higher AD than CF readers.

In CC5, no interactions between age and reading group were observed. However main effects of reading group were present for FA $F(2,46)=5.91$, $p<0.006$), MD $F(2,46)=3.42$, $p<0.05$), and RD $F(2,46)=5.03$, $p<0.02$). Planned group comparisons identified increases in FA for the DX group compared to both TDR $F(1,46)=4.57$, $p<0.04$) and CF $F(1,46)=10.69$,

p=0.002) groups. The TDR group had higher RD than both the DX $F(1,46)=10.0$, $p<0.003$) and CF $F(1,46)=5.04$, $p<0.03$) groups. MD differed only between the DX and CF groups, with the DX readers having lower MD $F(1,46)=6.83$, $p<0.02$).

Main effects of age on segment volume were observed for CC4 $F(1,46)=4.11$, $p<0.05$), CC5 $F(1,46)=4.57$, $p<0.04$), and CC7 $F(1,46)=4.92$, $p<0.04$), however none of these age effects interacted with reading groups.

Age Dependence of the Macro and Microstructure attributes of the CC

As a quality assurance measure and to help visualize the sources of variance in the macrostructural and microstructural attributes of the CC we plotted a scatter of the three reading groups as function of age. Figure 3A shows that the CC normalized area increases with age in the entire CC ($r=0.305$; $p=0.03$; $N=50$) and CC5 ($r=0.32$; $p=0.02$; Fig. 3B). The radial diffusivity decreased slowly with age in the splenium ($r=-0.25$; $r=0.08$; Fig. 3C) whereas the axial diffusivity weakly correlated with age ($r=0.005$; $p=0.97$; Fig. 3D).

Correlation between the Macro and Microstructural Measures of the CC and Reading

Because sCC and CC5 showed significant differences on the microstructural attributes, we show the CC attribute correlations with the Letter Word ID with and without age adjustments in Figure 4. Fig. 4A shows insignificant correlations of Letter Word ID with the ICV-normalized entire CC area ($r=-0.189$; $p=0.19$) and sCC ($r=-0.209$; $p=0.15$; Fig. 4B). Average mean diffusivity in CC5 correlated positively with Letter Word ID ($r=0.349$; $p=0.01$; Fig. 4C) while FA (CC5) correlated negatively with Letter Word ID ($r=0.387$; $p=0.006$; Fig. 4D). These correlations are better explained by a strong correlation with radial diffusivity in CC5 ($r=0.380$; $p=0.007$; Fig. 4E) compared with the axial diffusivity ($r=0.274$; $p=0.06$; Fig. 4F)

DISCUSSION

The human midsagittal CC offers an ideal compact structure to study *in vivo* white matter connectivity in both health and disease. The CC has been the focus of several MRI and postmortem histological reports (2, 12). It is commonly believed that the area of the CC may be related to the number and microstructure of the axons traversing the sagittal midline (1, 2). This assumption may be most valid in the anterior CC where small-caliber axons are thinly-myelinated and densely-packed (12). Contributors to callosal area in other regions may include axons with different myelin, size and shape distributions in addition to glia support cells. Anterior callosal axons interconnect certain frontal gray matter cortices where processing is slower than that of the posterior and parietal regions (2, 12, 19).

To the best of our knowledge, this is the first application of DTI-based and validated midsagittal callosal segmentation methods to examine the role of CC in reading disabilities in children using cross-sectional areas and their corresponding microstructural DTI attributes. Our finding of enlarged normalized CC splenial cross-sectional area in dyslexics is consistent with previous reports in children (30–35). The increase in average FA (CC5) in children with dyslexia compared to healthy controls is consistent with several previous DTI reports on reading impairment and using different methods that include DTI tractography (51–53). An abnormal increase in FA in patient populations has also been reported in several developmental disorders, including Turner and William’s syndromes (54).

Since FA is a derived mathematical metric that can be expressed as a function of the ratio of axial-to-radial diffusivities (55–58), it must be remembered that it has no simple biophysical correlate (59). The contributors to diffusion anisotropy in white matter have not yet been resolved even on compact structures such as the CC (9, 10). Diffusion anisotropy in white

matter has been reported in unmyelinated structures and has been attributed to several contributors (59) that include axonal membranes, intravoxel coherence (60), intraxonal microstructure (61), myelination and other biophysical factors (59, 62, 63).

Reading group differences were most pronounced in the CC5 cross-sectional segment. FA was significantly higher in DX group whereas MD and RD were significantly reduced relative to TDRs. The CF group exhibited similar characteristics to the TDRs in measures of FA, MD, and AD. However, RD was significantly decreased in both DX and CF readers, compared to TDRs. These group differences may be explained by increased myelin in segment CC5 of reading disabled children. Similar changes have been observed in animal models of myelination (63) and stem cell therapy for white matter dysmyelination (64). The increase in CC5 cross-sectional area might also indicate an increase in axonal caliber (65).

Either an increase in CC5 myelination or axonal caliber suggests that the dyslexic brain is “wired” for increased inter-hemisphereic communication.

Our finding of positive correlation of reading scores in CC5 mean diffusivity and negative correlation of FA may appear paradoxical at a glance, but these observations are consistent with previous reports on adults and children using fiber tractography (51–53). The direction of increase of Letter Word ID with both axial and radial diffusivities may be hypothesized to relate to the dynamic changes in axonal caliber or intra axonal diffusivity (59, 65).

Increases in myelination and/or axonal caliber in the CC5 segment may enhance communication between the two hemispheres and could reflect re-wiring due to recruitment of additional brain regions during processing of written language.

Acknowledgments

This work is funded by the American National Institutes of Health (NIH)- Institute for Neurological Diseases and Stroke (NIH-NINDS: R01-NS052505-04) awarded to KMH, NIH-Child Health and Development (NICHD) and P01-HD35946 awarded to JMF. The purchase of the 3.0 T MRI clinical scanner was partially funded by NIH grant S10 RR19186 awarded to PAN. The authors wish to thank Vipul Kumar Patel for helping in data acquisition.

Abbreviations

AD,MD, RD	axial, mean and radial diffusivities, respectively
CC	corpus callosum
CCA	corpus callosum midsagittal cross-sectional area
eCC	entire CC
cMRI	conventional MRI
D_{av}	average or mean diffusivity
DTI	diffusion tensor imaging
FA	fractional anisotropy
qMRI	quantitative MRI

References

1. Cook, ND. The Brain Code: mechanisms of information transfer and the role of the corpus callosum. Cook ND; London: 1986.
2. Zaidel, E.; Iacoboni, M. The parallel brain: The Cognitive Neuroscience of the Corpus Callosum. MIT press; Cambridge: 2003.

3. Rakic P, Yakovlev PI. Development of the corpus callosum and cavum septi in man. J Comp Neurol. 1968; 132:45–72. [PubMed: 5293999]

4. De Lacoste MC, Kirkpatrick JB, Ross ED. Topography of the human corpus callosum. J Neuropathol Exp Neurol. 1985; 44:578–591. [PubMed: 4056827]

5. Rauch RA, Jinkins JR. Analysis of cross-sectional area measurements of the corpus callosum adjusted for brain size in male and female subjects from childhood to adulthood. Behav Brain Res. 1994; 64:65–78. [PubMed: 7840893]

6. Johnson SC, Farnworth T, Pinkston JB, Bigler ED, Blatter DD. Corpus callosum surface area across the human adult life span: effect of age and gender. Brain Research Bulletin. 1994; 35:373–377. [PubMed: 7850489]

7. McLaughlin NC, Paul RH, Grieve SM, Williams LM, Laidlaw D, Dicarlo M, Clark CR, Whelihan W, Cohen RA, Whitford TJ, Gordon E. Diffusion tensor imaging of the corpus callosum: a cross-sectional study across the lifespan. Int J Dev Neurosci. 2007; 25:215–221. [PubMed: 17524591]

8. Hasan KM, Ewing-Cobbs L, Kramer LA, Fletcher JM, Narayana PA. Diffusion tensor quantification of the macrostructure and microstructure of human midsagittal corpus callosum across the lifespan. NMR Biomed. 2008; 21:1094–1101. [PubMed: 18615857]

9. Hasan KM, Kamali A, Kramer LA, Papnicolaou AC, Fletcher JM, Ewing-Cobbs L. Diffusion tensor quantification of the human midsagittal corpus callosum subdivisions across the lifespan. Brain Res. 2008; 1227:52–67. [PubMed: 18598682]

10. Hasan KM, Kamali A, Iftikhar A, Kramer LA, Papanicolaou AC, Fletcher JM, Ewing-Cobbs L. Diffusion tensor tractography quantification of the human corpus callosum fiber pathways across the lifespan. Brain Res. 2009; 1249:91–100. [PubMed: 18996095]

11. Lebel C, Caverhill-Godkewitsch S, Beaulieu C. Age-related regional variations of the corpus callosum identified by diffusion tensor tractography. Neuroimage. 2010; 52:20–31. [PubMed: 20362683]

12. Aboitiz F, Scheibel AB, Fisher RS, Zaidel E. Fiber composition of the human corpus callosum. Brain Res. 1992; 598:143–153. [PubMed: 1486477]

13. Barkovich AJ, Norman D. Anomalies of the corpus callosum: correlation with further anomalies of the brain. AJNR Am J Neuroradiol. 1988; 151:71–79.

14. Laissy JP, Patrux B, Duchateau C, Hannequin D, Hugonet P, Ait-Yahia H, Thiebot J. Midsagittal MR measurements of the corpus callosum in healthy subjects and diseased patients: a prospective study. AJNR Am J Neuroradiol. 1993; 14:145–154. [PubMed: 8427077]

15. Giedd JN, Rumsey JM, Castellanos FX, Rajapakse JC, Kaysen D, Vaituzis AC, Vauss YC, Hamburger SD, Rapoport JL. A quantitative MRI study of the corpus callosum in children and adolescents. Brain Res Dev Brain Res. 1996; 91:274–280.

16. Keshavan MS, Diwadkar VA, DeBellis M, Dick E, Kotwal R, Rosenberg DR, Sweeney JA, Minshew N, Pettegrew JW. Development of the corpus callosum in childhood, adolescence and early adulthood. Life Sci. 2002; 70:1909–1922. [PubMed: 12005176]

17. Pujol J, Vendrell P, Junque C, Marti-Vilalta JL, Capdevila A. When does human brain development end? Evidence of corpus callosum growth up to adulthood. Ann Neurol. 1993; 34:71–75. [PubMed: 8517683]

18. Witelson SF, Goldsmith CH. The relationship of hand preference to anatomy of the corpus callosum in men. Brain Res. 1991; 545:175–182. [PubMed: 1860044]

19. Ringo JL, Doty RW, Demeter S, Simard PY. Time is of the essence: a conjecture that hemispheric specialization arises from interhemispheric conduction delay. Cereb Cortex. 1994; 4:331–43. Review. [PubMed: 7950307]

20. Steinmetz H, Staiger JF, Schlaug SG, Huang Y, Jäncke L. Inverse relationship between brain size and callosal connectivity. Naturwissenschaften. 1996; 83:221. [PubMed: 8668233]

21. Westerhausen R, Kreuder F, Dos Santos Sequeira S, Walter C, Woerner W, Wittling RA, Schweiger E, Wittling W. The association of macro- and microstructure of the corpus callosum and language lateralisation. Brain Lang. 2006; 97:80–90. [PubMed: 16157367]

22. Wahl M, Lauterbach-Soon B, Hattingen E, Jung P, Singer O, Volz S, Klein JC, Steinmetz H, Ziemann U. Human motor corpus callosum: topography, somatotopy, and link between microstructure and function. J Neurosci. 2007; 27:12132–12138. [PubMed: 17989279]

23. Luders E, Narr KL, Bilder RM, Thompson PM, Szeszko PR, Hamilton L, Toga AW. Positive correlations between corpus callosum thickness and intelligence. Neuroimage. 2007; 37:1457–1464. [PubMed: 17689267]
24. Bengtsson SL, Nagy Z, Skare S, Forsman L, Forssberg H, Ullén F. Extensive piano practicing has regionally specific effects on white matter development. Nat Neurosci. 2005; 8:1148–1150. [PubMed: 16116456]
25. Paul LK. Developmental malformation of the corpus callosum: a review of typical callosal development and examples of developmental disorders with callosal involvement. J Neurodev Disord. 2011; 3:3–27. [PubMed: 21484594]
26. Alexander AL, Lee JE, Lazar M, Boudos R, DuBray MB, Oakes TR, Miller JN, Lu J, Jeong EK, McMahon WM, Bigler ED, Lainhart JE. Diffusion tensor imaging of the corpus callosum in Autism. Neuroimage. 2007; 34:61–73. [PubMed: 17023185]
27. Highley JR, Esiri MM, McDonald B, Cortina-Borja M, Herron BM, Crow TJ. The size and fibre composition of the corpus callosum with respect to gender and schizophrenia: a post-mortem study. Brain. 1999; 122:99–110. [PubMed: 10050898]
28. Evangelou N, Konz D, Esiri MM, Smith S, Palace J, Matthews PM. Regional axonal loss in the corpus callosum correlates with cerebral white matter lesion volume and distribution in multiple sclerosis. Brain. 2000; 123:1845–1849. [PubMed: 10960048]
29. Wiltshire K, Foster S, Kaye JA, Small BJ, Camicioli R. Corpus callosum in neurodegenerative diseases: findings in Parkinson's disease. Dement Geriatr Cogn Disord. 2005; 20:345–351. [PubMed: 16192724]
30. Larsen JP, Höien T, Ödegaard H. Magnetic resonance imaging of the corpus callosum in developmental dyslexia. Cogn Neuropsychol. 1992; 9:123–134.
31. Hynd GW, Hall J, Novey ES, Eliopulos D, Black K, Gonzalez JJ, Edmonds JE, Riccio C, Cohen M. Dyslexia and corpus callosum morphology. Arch Neurol. 1995; 52:32–8. [PubMed: 7826273]
32. Robichon F, Habib M. Abnormal callosal morphology in male adult dyslexics: Relationships to handedness and phonological abilities. Brain Lang. 1998; 62:127–146. [PubMed: 9570883]
33. von Plessen K, Lundervold A, Duta N, Heiervang E, Klauschen F, Smievoll AI, Ersland L, Hugdahl K. Less developed corpus callosum in dyslexic subjects--a structural MRI study. Neuropsychologia. 2002; 40:1035–1044. [PubMed: 11900755]
34. Robichon F, Bouchard P, Démonet J, Habib M. Developmental dyslexia: re-evaluation of the corpus callosum in male adults. Eur Neurol. 2000; 43:233–237. [PubMed: 10828655]
35. Robichon F, Levrier O, Farnarier P, Habib M. Developmental dyslexia: atypical cortical asymmetries and functional significance. Eur J Neurol. 2000; 7:35–46. [PubMed: 10809913]
36. Frye RE, Hasan K, Xue L, Strickland D, Malmberg B, Liederman J, Papanicolaou A. Splenium microstructure is related to two dimensions of reading skill. Neuroreport. 2008; 19:1627–1631. [PubMed: 18806688]
37. Fletcher JM. Dyslexia: The evolution of a scientific concept. Journal of the International Neuropsychological Society. 2009; 15:501–508. [PubMed: 19573267]
38. Shaywitz SE, Shaywitz BA. Dyslexia (specific reading disability). Biol Psychiatry. 2005; 57:1301–1309. [PubMed: 15950002]
39. Shaywitz SE, Shaywitz BA. Paying attention to reading: the neurobiology of reading and dyslexia. Dev Psychopathol. 2008; 20:1329–1349. Review. [PubMed: 18838044]
40. Beaulieu C, Plewes C, Paulson LA, Roy D, Snook L, Concha L, Phillips L. Imaging brain connectivity in children with diverse reading ability. Neuroimage. 2005; 25:1266–1271. [PubMed: 15850744]
41. Sun YF, Lee JS, Kirby R. Brain imaging findings in dyslexia. Pediatr Neonatol. 2010; 51:89–96. Review. [PubMed: 20417459]
42. Rimrodt SL, Clements-Stephens AM, Pugh KR, Courtney SM, Gaur P, Pekar JJ, Cutting LE. Functional MRI of sentence comprehension in children with dyslexia: beyond word recognition. Cereb Cortex. 2009; 19:402–413. [PubMed: 18515796]
43. Woodcock, R.; Mather, N. Woodcock-Johnson Tests of Achievement. Riverside; Itasca, IL: 2001.
44. Woodcock, RW. Woodcock reading master tests-revised. American Guidance Service; Circle Pines, MN: 1998.

45. Kaufman, AS.; Kaufman, NL. Kaufman Brief Intelligence Test. 2. Pearson; San Antonio: 2004.
46. Torgesen, J.; Wagner, R.; Rashotte, C. Test of Word Reading Efficiency (TOWRE). Pro- Ed Incorporated; Austin, TX: 1999.
47. Thorndike, R.; Hagen, E.; Sattler, J. The Stanford-Binet Intelligence Test. 4. Riverside; Itasca, IL: 1986.
48. Hasan KM, Narayana PA. Computation of the fractional anisotropy and mean diffusivity maps without tensor decoding and diagonalization: Theoretical analysis and validation. Magn Reson Med. 2003; 50:589–598. [PubMed: 12939767]
49. Hasan KM. A framework for quality control and parameter optimization in diffusion tensor imaging: theoretical analysis and validation. Magn Reson Imaging. 2007; 25:96–112.
50. Glantz, SA. Primer of biostatistics. 5. McGraw-Hill; New York: 2002.
51. Dougherty RF, Ben-Shachar M, Deutsch GK, Hernandez A, Fox GR, Wandell BA. Temporal-callosal pathway diffusivity predicts phonological skills in children. Proc Natl Acad Sci U S A. 2007; 104:8556–8561. [PubMed: 17483487]
52. Frye RE, Liederman J, Hasan KM, Lincoln A, Malmberg B, McLean J 3rd, Papanicolaou A. Diffusion tensor quantification of the relations between microstructural and macrostructural indices of white matter and reading. Hum Brain Mapp. 2011; 32:1220–1235. [PubMed: 20665719]
53. Yeatman JD, Dougherty RF, Rykhlevskaia E, Sherbondy AJ, Deutsch GK, Wandell BA, Ben-Shachar M. Anatomical properties of the arcuate fasciculus predict phonological and reading skills in children. J Cogn Neurosci. 2011; 23:3304–3317. [PubMed: 21568636]
54. Hoeft F, Barnea-Goraly N, Haas BW, Golarai G, Ng D, Mills D, Korenberg J, Bellugi U, Galaburda A, Reiss AL. More is not always better: increased fractional anisotropy of superior longitudinal fasciculus associated with poor visuospatial abilities in Williams syndrome. J Neurosci. 2007; 27:11960–11965. [PubMed: 17978036]
55. Hasan KM, Alexander AL, Narayana PA. Does fractional anisotropy have better noise immunity characteristics than relative anisotropy in diffusion tensor MRI? An analytical approach. Magn Reson Med. 2004; 51:413–417. [PubMed: 14755670]
56. Hasan KM, Narayana PA. Retrospective measurement of the diffusion tensor eigenvalues from diffusion anisotropy and mean diffusivity in DTI. Magn Reson Med. 2006; 56:130–137. [PubMed: 16755537]
57. Hasan KM, Basser PJ, Parker DL, Alexander AL. Analytical computation of the eigenvalues and eigenvectors in DT-MRI. J Magn Reson. 2001; 152:41–47. [PubMed: 11531362]
58. Walimuni IS, Hasan KM. Atlas-based investigation of human brain tissue microstructural spatial heterogeneity and interplay between transverse relaxation time and radial diffusivity. Neuroimage. 2011; 57:1402–1410. [PubMed: 21658457]
59. Beaulieu C. The basis of anisotropic water diffusion in the nervous system - a technical review. NMR Biomed. 2002; 15:435–455. [PubMed: 12489094]
60. Takahashi M, Ono J, Harada K, Maeda M, Hackney DB. Diffusional anisotropy in cranial nerves with maturation: quantitative evaluation with diffusion MR imaging in rats. Radiology. 2000; 216:881–885. [PubMed: 10966726]
61. Kinoshita Y, Ohnishi A, Kohshi K, Yokota A. Apparent diffusion coefficient on rat brain and nerves intoxicated with methylmercury. Environ Res. 1999; 80:348–354. [PubMed: 10330308]
62. Song SK, Yoshino J, Le TQ, Lin SJ, Sun SW, Cross AH, Armstrong RC. Demyelination increases radial diffusivity in corpus callosum of mouse brain. Neuroimage. 2005; 26:132–140. [PubMed: 15862213]
63. Drobyshevsky A, Song SK, Gamkrelidze G, Wyrwicz AM, Derrick M, Meng F, Li L, Ji X, Trommer B, Beardsley DJ, Luo NL, Back SA, Tan S. Developmental changes in diffusion anisotropy coincide with immature oligodendrocyte progression and maturation of compound action potential. J Neurosci. 2005; 25:5988–5997. [PubMed: 15976088]
64. McGraw P, Liang L, Escolar M, Mukundan S, Kurtzberg J, Provenzale JM. Krabbe disease treated with hematopoietic stem cell transplantation: serial assessment of anisotropy measurements--initial experience. Radiology. 2005; 236:221–230. [PubMed: 15987975]
65. Paus T. Growth of white matter in the adolescent brain: myelin or axon? Brain Cogn. 2010; 72:26–35. [PubMed: 19595493]

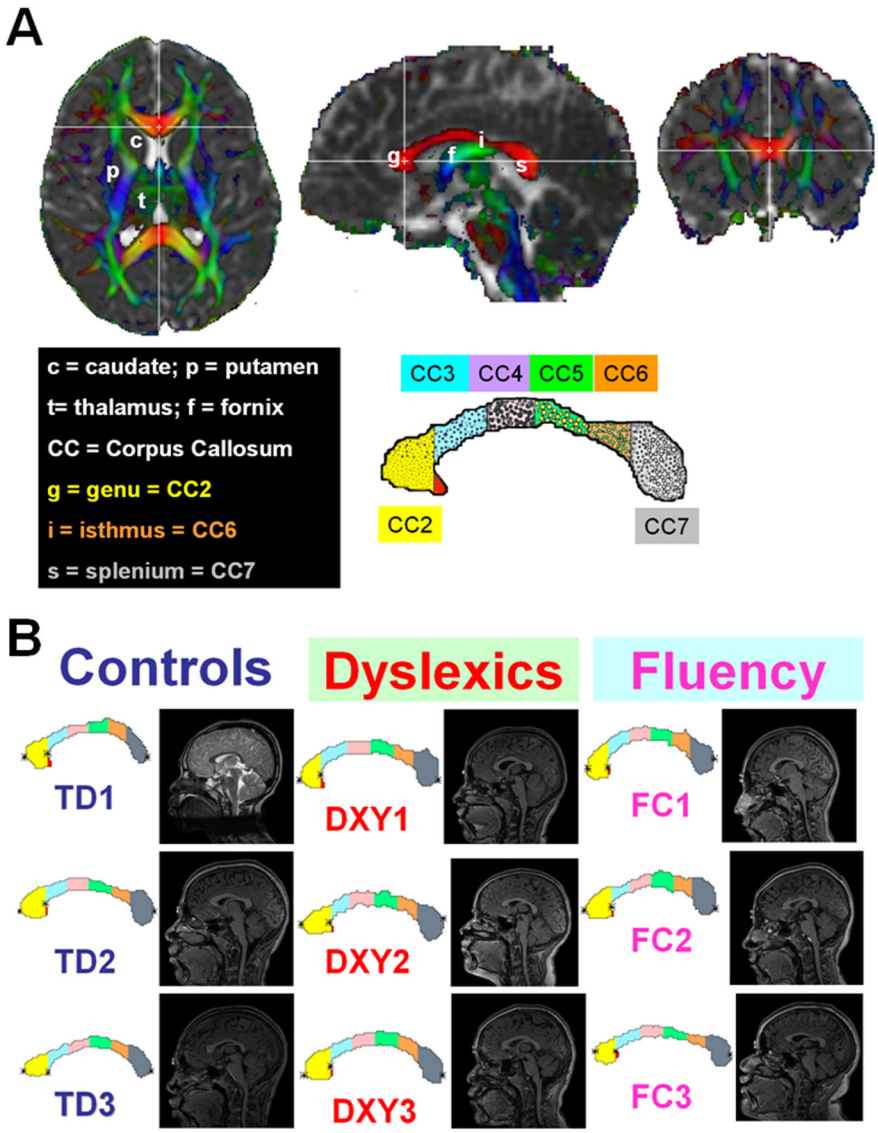

Figure 1.
(A) Illustration of corpus callosum DTI-segmentation method and (B) application to the three groups in our study (three representative children from the healthy developing, and children with developmental reading (dyslexia) and fluency or comprehension difficulties.

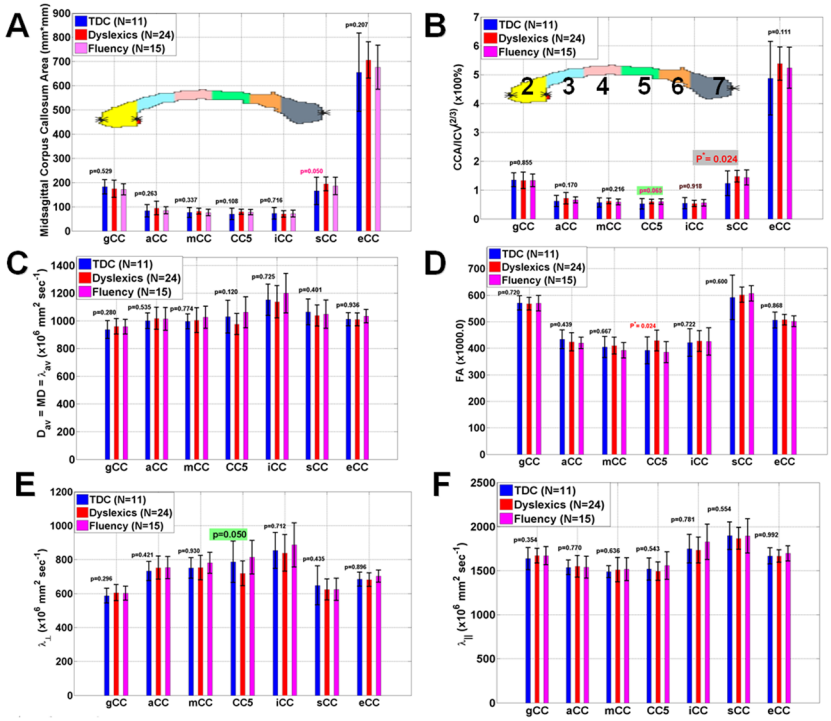

Figure 2.

Bar graphs of showing mean and standard deviations of the three groups of the callosal (A) midsagittal cross-sectional areas (B) normalized callosal areas ($CCA/ICV^{2/3}$) (C) Mean diffusivity (D) fractional anisotropy (E) radial diffusivity and (F) axial diffusivity.

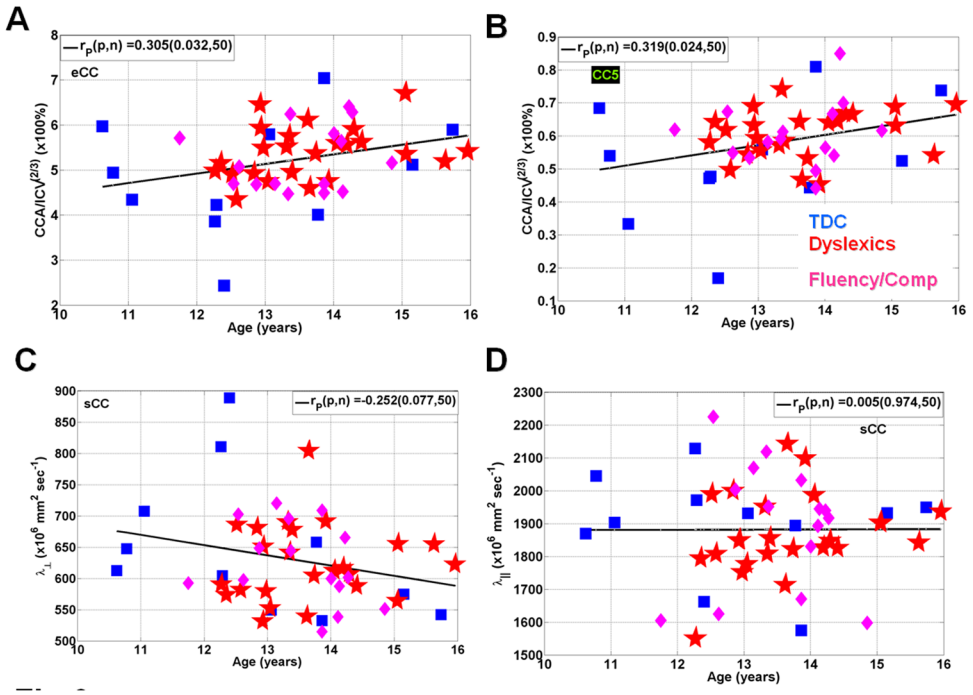

Figure 3.

Representative scatter plots and linear regression for the three groups of age vs. (A) normalized callosal area (B) normalized CC5 areas (C) radial diffusivity in the splenium and (D) axial diffusivity in the splenium.

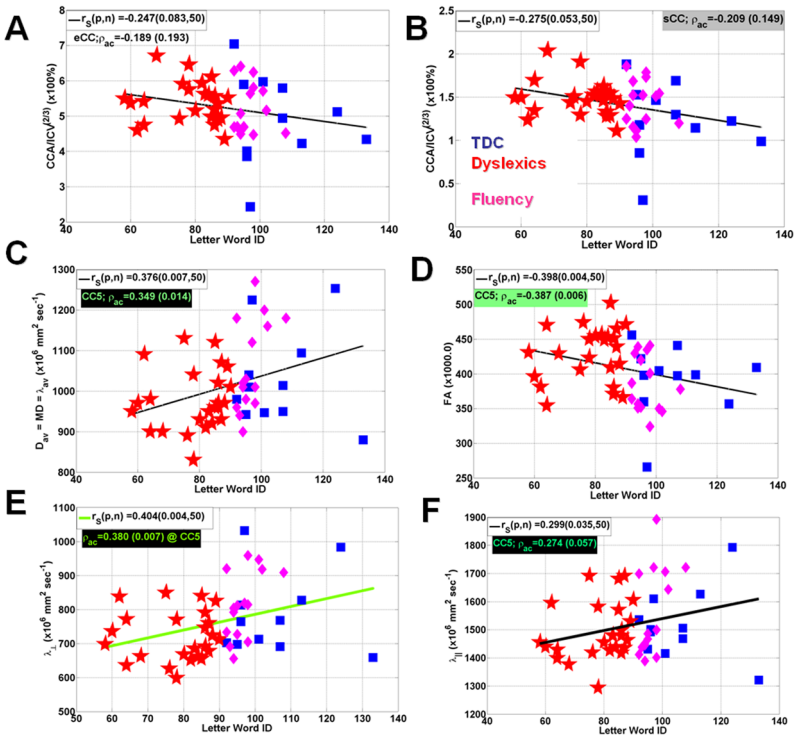

Figure 4.

Representative scatter plots and linear regression analysis for the three groups Letter Word ID scores vs. (A) Normalized entire CC midsagittal area (B) normalized splenium area (C) average mean diffusivity in CC5 (D) average FA in CC5 (E) average radial diffusivity in CC5 and (F) average radial diffusivity in CC5.

Table 1

Mean (MN) and standard deviation (SD) values of composite IQ, Letter word ID, passage comprehension and Test of Word Reading Efficiency (TOWRE), ICV and entire CC area measurements on healthy controls, dyslexics and the Comprehension/Fluency groups.

	Typically Dev. Readers (TD)	Dyslexics (DX)	Fluency/Comp (FC)	p (TD, DX)	p (TD, FC)
N(F; LH)	11 (3; 2M)	24 (11; 1F/2M)	15 (9; 0)		
Age (years)					
Mean ± S.D.	12.8 ± 1.7	13.7 ± 1.0	13.5 ± 0.8	0.07	0.66
Range [Min-to-Max]	10.6–15.7	12.3–16.0	11.7–14.9		
Composite IQ	103.8 ± 8.7	87.2 ± 10.9	98.5 ± 9.2	**0.0002**	0.16
	87–113 (N=10)	69–104 (N=23)	81–110		
Letter	105.5 ± 13.1	78.4 ± 10.2	96.7 ± 4.4	**1×10^{-7}**	**0.02**
Word ID	92–133	58–90	92–108		
Passage	101.8 ± 10.2	79.5 ± 12.8	90.1 ± 8.4	**1.5×10^{-5}**	**0.004**
Comprehension	90–124	53–99	76–108		
ICV (cm^3=mL)	1570.3 ± 83.6	1508.0 ± 127.8	1477.5 ± 182.2	0.15	0.13
	1449.0–1662.8	1263.0–1740.4	1149.2–1747.4		
eCCA (mm^2)	655.6 ± 161.8	706.6 ± 74.9	676.2 ± 91.3	0.21	0.68
	341.0–901.8	537.0–854.3	547.6–833.2		